

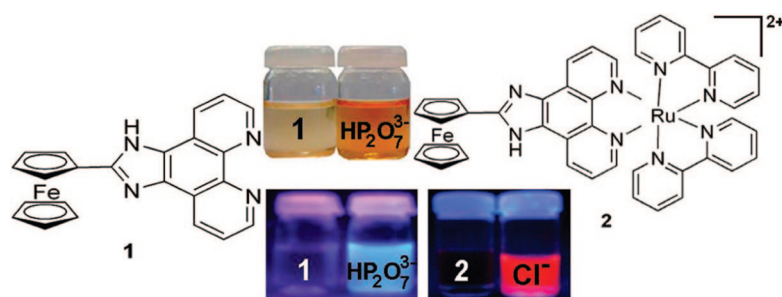
Cation Coordination Induced Modulation of the Anion Sensing Properties of a Ferrocene–Imidazophenanthroline Dyad: Multichannel Recognition from Phosphate-Related to Chloride Anions

Fabiola Zapata, Antonio Caballero, Arturo Espinosa, Alberto Tárraga,* and Pedro Molina*

Departamento de Química Orgánica, Facultad de Química, Universidad de Murcia, Campus de Espinardo, E-30100 Murcia, Spain

pmolina@um.es; atarraga@um.es

Received February 5, 2008



A new chemosensor molecule **1** based on a ferrocene-imidazophenanthroline dyad, effectively recognizes aqueous hydrogenpyrophosphate and the organic anions ADP and ATP through three different channels. A cathodic shift of the ferrocene/ferrocenium oxidation wave ($\Delta E_{1/2}$ ranging from -130 mV for hydrogenpyrophosphate and fluoride to -40 mV for ADP). A progressive red-shift of the absorption bands and/or appearance of a new low energy band at 314–319 nm. These changes in the absorption spectra are accompanied by color changes from pale yellow to orange or pink, which allow the potential for “naked eye” detection. The emission spectrum ($\lambda_{\text{exc}} = 390$ nm) undergoes an important chelation-enhanced fluorescence effect (CHEF = 50) in the presence of 2.5 equiv of hydrogenpyrophosphate anion and with a large excess of fluoride anion (CHEF = 114). Interestingly, the emission spectrum obtained at different excitation energy ($\lambda_{\text{exc}} = 340$ nm) in the presence of AcOH acid is red-shifted and not only perturbed by the hydrogenpyrophosphate anion (CHEF = 71) but also with the organic anions ATP (CHEF = 25), ADP (CHEF = 15), and the dihydrogenphosphate (CHEF = 25). The stable heterobimetallic ruthenium (II) complex **2** selectively senses the chloride anion over other anions examined through two channels: cathodic redox shift ($\Delta E_{1/2} = -80$ mV) of the Fe(II)/Fe(III) redox couple keeping the oxidation wave of the ruthenium (II) center unchanged and a significant red emission enhancement (CHEF = 30). ¹H and ³¹P NMR studies as well as DFT calculations have been carried out to get information about which molecular sites are involved in bonding. About the deprotonation/coordination dualism, the combined electrochemical, absorption, emission, and NMR data strongly support that fluoride anion induces only deprotonation, anions dihydrogenphosphate, ATP, and ADP from hydrogen-bonded complexes and formation of hydrogen-bonded complex between receptor **1** and hydrogenpyrophosphate anion and deprotonation proceed simultaneously. In regards to receptor **2**, all available data (electrochemical, absorption, emission, and ¹H NMR) strongly support the formation of a [2·Cl⁻] hydrogen-bonded complex.

Introduction

The design and synthesis of receptors and chemosensors capable of binding and sensing anions selectively has attracted much attention in recent years because of the fundamental role of anions in a wide range of biological and chemical processes.¹

A wide variety of receptors that utilize electrostatic interactions, hydrogen bond donor groups, Lewis acid groups, and

(1) Sessler, J. L.; Gale, P. A.; Cho, W. S. In *Anion Receptor Chemistry*; Monographs in Supramolecular Chemistry; Stoddart, J. F., Ed.; RSC: Cambridge, 2006.

hydrophobic interactions have been employed to bind anionic guest species over the intervening years.² In this context, simple coordination compounds containing a combination of positive charge and monodentate ligands featuring hydrogen bond donor groups provide the basis for powerful molecular sensors for anions and have recently received much interest among researchers.³

To date, several different heterocyclic ring systems containing a pyrrolic NH group have been reported in the literature as hydrogen-bond donors to anions, as demonstrated in calixpyrroles,⁴ expanded porphyrinoids,⁵ pyrrole derivatives,⁶ indoles,⁷ bisindoles,⁸ bisimidazoles,⁹ indolocarbazoles,¹⁰ and benzimidazoles.¹¹ Surprisingly, although the imidazo[4,5-*f*]-1,10-phenanthroline moiety has been employed frequently to form ruthenium (II) polypyridyl complexes¹² using the two nitrogen atoms of the bipyridine fragment, as far as we know no anion receptors making use of the NH group of the imidazole ring system have ever been reported.¹³

Sensing of a fluoride anion, the smallest anion, has attracted growing attention due to its beneficial effects (e.g., prevention of dental caries) and detrimental (e.g., fluorosis) roles.¹⁴ The conventional binding approaches have used either designed hydrogen bonding or the specific strong affinity of a boron atom toward the fluoride anion. These binding events have been converted into an electrochemical¹⁵ or fluorescent¹⁶ change or, more directly, a colorimetric change detectable by the naked

eye.¹⁷ Anions such as pyrophosphate and adenosine triphosphate (ATP) play an important role in energy transduction in organism and control metabolic processes by participation in enzymatic reactions. ATP hydrolysis with the concomitant release of pyrophosphate is central to many biochemical reactions, such as DNA polymerization and the synthesis of cyclic adenosine monophosphate (c-AMP) catalyzed by DNA polymerase and adenylate cyclase, respectively.¹⁸ Furthermore, the detection of released pyrophosphate has been examined as a real-time DNA sequencing method,¹⁹ and it has also been considered important in cancer research.²⁰ Therefore, the detection and discrimination of these anions has been the main focus of the effort of several research groups. However, very few examples of effective selective fluorescent,²¹ chromogenic,²² or redox²³ chemosensors have so far been reported.

Only in recent years have alternative mechanisms for several types of anion-receptor interaction been developed.²⁴ If the basicity of the anion is insufficient to induce deprotonation of the receptor, one observes formation of a hydrogen-bonded complex manifested in a red-shift of the receptor absorption band and a downfield shift or often disappearance of NMR signals of the receptors protons involved in the hydrogen bonding. If the basicity of the anion is high enough to deprotonate the receptor, one observes the appearance of a new intense absorption band in the visible region of the electronic spectrum, the disappearance of NMR signals of abstracted

(2) For reviews, see: (a) Beer, P. D.; Gale, P. A. *Angew. Chem., Int. Ed.* **2001**, *40*, 486–516. (b) Bondy, C. R.; Loeb, S. J. *Coord. Chem. Rev.* **2003**, *240*, 77–99. (c) Choi, K.; Hamilton, A. D. *Coord. Chem. Rev.* **2003**, *240*, 101–110. (d) Gale, P. A. *Coord. Chem. Rev.* **2003**, *240*, 191–221. (e) Suksai, C.; Tuntulani, T. *Chem. Soc. Rev.* **2003**, *32*, 192–202. (f) Bowman-James, C. *Acc. Chem. Res.* **2005**, *38*, 671–678. (g) Wiskur, S. L.; Ait-Haddou, H.; Lavigne, J. J.; Anslly, E. *Acc. Chem. Res.* **2001**, *34*, 963–972. (h) Sessler, J. L.; Davis, J. M. *Acc. Chem. Res.* **2001**, *34*, 989–997. (i) Yoon, J.; Kim, S.; Singh, N. J.; Kim, K. S. *Chem. Soc. Rev.* **2006**, *35*, 355–360. (j) Gale, P. A. *Acc. Chem. Res.* **2006**, *39*, 465–475.

(3) For review, see: (a) Pérez, J.; Riera, L. *Chem. Commun.* **2008**, 533–543. (4) (a) Anzenbacher, P.; Jursiková, K.; Sessler, J. L. *J. Am. Chem. Soc.* **2000**, *122*, 57102. (b) Nielsen, K. A.; Cho, W.-S.; Jeppesen, J. O.; Lynch, V. M.; Becher, J.; Sessler, J. L. *J. Am. Chem. Soc.* **2004**, *126*, 16296–16297. (d) Sessler, J. L.; Katayev, E.; Pantos, G. D.; Scherbakov, P.; Reshetova, M. D.; Khrestalev, V. N.; Lynch, V. M.; Ustynyuk, Y. A. *J. Am. Chem. Soc.* **2005**, *127*, 11442–11446.

(5) For reviews, see: (a) Sessler, J. L.; Davis, J. M. *Acc. Chem. Res.* **2001**, *34*, 989–997. (b) Sessler, J. L.; Camiolo, S.; Gale, P. A. *Coord. Chem. Rev.* **2003**, *240*, 17–55.

(6) (a) Lin, C.-I.; Selvi, S.; Fang, J.-M.; Chou, P.-T.; Kai, C. H.; Cheng, Y.-Y. *J. Org. Chem.* **2007**, *72*, 3537–3542. (b) Sessler, J. L.; Dan Pantos, G.; Gale, P. A.; Light, M. E. *Org. Lett.* **2006**, *8*, 1593–1596. For reviews, see: (c) Gale, P. A. *Chem. Commun.* **2005**, 3761–3772.

(7) Pfeffer, F. M.; Lim, K. F.; Sedgwick, *Org. Biomol. Chem.* **2007**, *5*, 1759–1799.

(8) Chang, K.-J.; Moon, D.; Lah, M. S.; Jeong, K.-S. *Angew. Chem., Int. Ed.* **2005**, *44*, 7926–7929.

(9) Causey, C. P.; Allen, W. E. *J. Org. Chem.* **2002**, *67*, 5963–5968.

(10) Curiel, D.; Cowley, A.; Beer, P. D. *Chem. Commun.* **2005**, 236–238.

(11) Kang, J.; Kim, H. S.; Jang, D. O. *Tetrahedron Lett.* **2005**, *46*, 6079–6082.

(12) Han, M.-J.; Gao, L.-H.; Wang, K.-Z. *New J. Chem.* **2006**, *30*, 208–214.

(13) Such as family of heterocyclic compounds has been used in the studies on the interaction between transition-metal complexes and DNA: (a) Xiong, Y.; Ji, L.-N. *Coord. Chem. Rev.* **1999**, *185–186*, 711–733. (b) Ji, L.-N.; Zou, X.-H.; Liu, J.-G. *Coord. Chem. Rev.* **2001**, *216–217*, 513–536. Only a ruthenium(II) complex of this ring system has been reported as a selective fluorescent sensor of Mg²⁺ cations: (c) Liu, Y.; Duan, Z.-Y.; Zhang, H.-Y.; Jiang, X.-L.; Han, J.-R. *J. Org. Chem.* **2005**, *70*, 1450–1455.

(14) Kirk, K. L. *Biochemistry of the Halogens and Inorganic Halides*; Plenum Press: New York, 1991; p 58

(15) (a) Desemund, C.; Sanyadanake, K. R. A. S.; Shinkai, S. *J. Chem. Soc., Chem. Commun.* **1995**, 333–334. (b) Yamamoto, H.; Ori, A.; Ueda, K.; Desemund, C.; Shinkai, S. *Chem. Commun.* **1996**, 407–408. (c) Otón, F.; Tárraga, A.; Molina, P. *Org. Lett.* **2006**, *8*, 2107–2110. (d) Otón, F.; Espinosa, A.; Tárraga, A.; Ramírez de Arellano, C.; Molina, P. *Chem.–Eur. J.* **2007**, *13*, 5742–5752.

(16) (a) Anzenbacher, P., Jr.; Try, A. C.; Miyaji, H.; Jursiková, K.; Lynch, V. M.; Marquez, M.; Sessler, J. L. *J. Am. Chem. Soc.* **2000**, *122*, 10268–10272. (b) Kima, T.-H.; Swager, T. M. *Angew. Chem., Int. Ed.* **2003**, *42*, 4803–4806. (c) Xu, G.; Tarr, M. A. *Chem. Commun.* **2004**, 1050–1051. (d) Wu, J.-S.; Zhou, J.-H.; Wang, P.-F.; Zhang, X.-H.; Wu, S.-K. *Org. Lett.* **2005**, *7*, 2133–2136. (e) Melaimi, M.; Gabbai, F. P. *J. Am. Chem. Soc.* **2005**, *127*, 9680–9681. (f) Kim, S. K.; Bok, J. H.; Bartsch, R. A.; Lee, J. Y.; Kim, J. S. *Org. Lett.* **2005**, *7*, 4839–4842. (g) Zhao, Y.-P.; Zhao, C.-C.; Wu, L.-Z.; Zhang, L.-P.; Tung, C.-H.; Pan, Y.-J. *J. Org. Chem.* **2006**, *71*, 2143–2149.

(17) (a) Miyaji, H.; Sato, W.; Sessler, J. L. *Angew. Chem., Int. Ed.* **2000**, *39*, 1777–1780. (b) Miyaji, H.; Sato, W.; Sessler, J. L.; Lynch, M. *Tetrahedron Lett.* **2000**, *41*, 1369–1373. (c) Miyaji, H.; Sessler, J. L. *Angew. Chem., Int. Ed.* **2001**, *40*, 154–157. (d) Yamaguchi, S.; Akiyama, S.; Tamao, K. *J. Am. Chem. Soc.* **2001**, *123*, 11372–11375. (e) Vazquez, M.; Fabbrizzi, L.; Taglietti, A.; Pedrido, R. M.; González-Noya, A. M.; Bermejo, M. R. *Angew. Chem., Int. Ed.* **2004**, *43*, 1962–1965. (f) Watanabe, S.; Seguchi, H.; Yoshida, K.; Kifune, K.; Tadaki, T.; Shiozaki, H. *Tetrahedron Lett.* **2005**, *46*, 8827–8829. (g) Lin, Z.-H.; Ou, S.-J.; Duan, C.-Y.; Zhang, B.-G.; Bai, Z.-P. *Chem. Commun.* **2006**, 624–626. (h) Ghosh, T.; Maiya, B. G.; Samanta, A. *Dalton Trans.* **2006**, 795–801.

(18) (a) Lipscombe, W. N.; Sträter, N. *Chem. Rev.* **1996**, *96*, 2375–2433. (b) Tabary, T.; Lu, L. *J. Immunol. Methods* **1992**, *156*, 55–60. (c) Nyrén, P. *Anal. Biochem.* **1987**, *167*, 235–238.

(19) Ronaghi, M.; Karamohamed, S.; Petterson, B.; Uhlen, M.; Nyren, P. *Anal. Biochem.* **1996**, *242*, 84–89.

(20) Xu, S.; He, M.; Yu, H.; Cai, X.; Tan, X.; Lu, B.; Shu, B. *Anal. Biochem.* **2001**, *299*, 188–193.

(21) (a) Fabbrizzi, L.; Marcotte, N.; Stomeo, F.; Taglietti, A. *Angew. Chem., Int. Ed.* **2002**, *41*, 3811–3814. (b) Gunnalagsson, T.; Davis, A. P.; O'Brien, J. E.; Glynn, M. *Org. Lett.* **2002**, *4*, 2449–2452. (c) Lee, D. H.; Kim, S. Y.; Hong, J.-I. *Angew. Chem., Int. Ed.* **2004**, *43*, 4777–4780. (d) Kanekiyo, Y.; Naganawa, R.; Tao, H. *Chem. Commun.* **2004**, 1006–1007. (e) Cho, H. K.; Lee, D. H.; Hong, J.-I. *Chem. Commun.* **2005**, 1690–1692. (f) Jang, Y. J.; Jun, E. J.; Lee, Y. J.; Kim, Y. S.; Kim, J. S.; Yoon, J. *J. Org. Chem.* **2005**, *70*, 9603–9606. (g) McDonough, M. J.; Reynolds, A. J.; Lee, W. Y. G.; Jolliffe, K. A. *Chem. Commun.* **2006**, 2971–2973. (h) Bazzicalupi, C.; Biagini, S.; Bencini, A.; Faggi, E.; Giorgi, C.; Matera, I.; Valtancoli, B. *Chem. Commun.* **2006**, 4087–4089. (i) Lee, H. N.; Swamy, K. M. K.; Kim, S. K.; Kwon, J.-Y.; Kim, Y.; Kim, S.-J.; Yoon, Y. J.; Yoon, J. *Org. Lett.* **2007**, *9*, 242–246. (j) Lee, H. N.; Xu, Z.; Kim, S. K.; Swamy, K. M. K.; Kim, Y.; Kim, S.-J.; Yoon, J. *J. Am. Chem. Soc.* **2007**, *129*, 3828–3829. (k) Swamy, K. M. K.; Kwon, S. K.; Lee, H. N.; Shantha Kumar, S. M.; Kim, J. S.; Yoon, J. *Tetrahedron Lett.* **2007**, *48*, 8683–8686.

(22) (a) Lee, D. H.; Im, J. H.; Son, S. U.; Young, K.; Hong, J.-I. *J. Am. Chem. Soc.* **2003**, *125*, 7752–7753. (b) Aldakov, D.; Anzenbacher, P., Jr. *J. Am. Chem. Soc.* **2004**, *126*, 4752–4753. (c) Nishiyabu, R., Jr. *J. Am. Chem. Soc.* **2005**, *127*, 8270–8271.

(23) Anzenbacher, P.; Palacios, M. A.; Kursikova, K.; Marquez, M. *Org. Lett.* **2005**, *7*, 5027–5030.

(24) Amendola, V.; Esteban-Gomez, D.; Fabbrizzi, L.; Licchelli, M. *Acc. Chem. Res.* **2006**, *39*, 343–353.

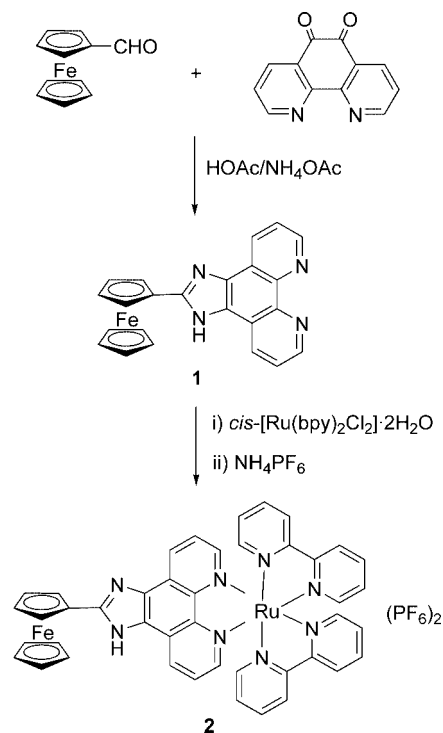
receptor protons, and an upfield shift of the signals of adjacent receptors protons.²⁵ More interestingly, some detailed studies have even suggested that mixed processes might occur: initial complex formation at low anion-to-receptor ratios, this then being followed by deprotonation at higher anion-to-receptor ratios.²⁶ The degree of deprotonation depends on the concentration of the receptor; as a result, a NMR titration may feel only hydrogen bonding, whereas a spectrophotometric titration may clearly show the deprotonation.²⁷ A simple way to measure the binding constant for the formation of the hydrogen-bonded complex is to perform the titration in the presence of added acid, which suppresses the deprotonation process.

Despite the development of these classical single-signaling approximations there is a paucity of use of multichannel signaling fluoride and pyrophosphate selective chemosensor molecules.²⁸ Generally, anion recognition motifs are often structurally complicated and require an elaborate and sophisticated synthetic process. Therefore, the development of simple and easy-to-make chemosensor molecules for anions is strongly desired. From this perspective, we decided to study a new type of anionophores by combining the redox activity of the ferrocene moiety with the strong hydrogen-bonding ability of the imidazole ring and the photoactive behavior of the phenanthroline ring. Here, we now report on chemosensor molecules **1** and **2** comprising an imidazophenanthroline ring, in which the fluorophore and the anion and cation binding sites are integrated into this ring system, which is linked to a redox-active ferrocene moiety to generate strong fluorescent, optical, and electrochemical signals.

Results and Discussion

Synthesis. Compound **1** was prepared in excellent yield by condensation of 1,10-phenanthroline-5,6-dione with formylferrocene in the presence of NH_4OAc , following an improved

SCHEME 1. Synthesis of Ligands **1** and **2**



modification of the previously reported method for related compounds.²⁹ Heterobimetallic ligand **2** was obtained in 70% yield from the reaction of **1** with *cis*-dichlorobis(2,2'-bipyridine)ruthenium(II) dihydrate and further treatment with NH_4PF_6 (Scheme 1).

Anion Sensing Properties. The binding and recognition ability of receptors **1** and **2** toward various anions (F^- , Cl^- , Br^- , AcO^- , NO_3^- , HSO_4^- , H_2PO_4^- , and $\text{HP}_2\text{O}_7^{3-}$), in the form of their corresponding tetrabutylammonium salts (TBA^+), and the organic anions ATP and ADP were evaluated by cyclic (CV) and Osteryoung square-wave voltammetry (OSWV).²⁶ The CV response of **1** in CH_3CN , also containing 0.1 M TBAPF_6 as supporting electrolyte, showed a reversible one-electron oxidation process at $E_{1/2} = 0.64$ V vs decamethylferrocene (DMFc) redox couple. The heterobimetallic ligand **2** displays a similar reversible oxidation process at $E_{1/2} = 0.67$ V vs DMFc, arising from the one-electron oxidation of the ferrocene unit, and two irreversible oxidative processes at approximately 1.40 and 1.45 V vs DMFc associated to the oxidations of the Ru center.

On stepwise addition of F^- anion to a solution of receptor **1** in CH_3CN , a clear evolution of the oxidation wave to $E_{1/2} = 0.57$ V ($\Delta E_{1/2} = -70$ mV) was observed with 1 equiv of added F^- anion. The electrochemical shift was accompanied by a decrease in current intensity, a behavior attributed to the formation of a complex with a lower diffusion coefficient.³⁰ OSWV titration also showed a measurable change in the peak current and oxidation potential (Figure 1a). Titration isotherms obtained from these changes were fitted nicely to a 1:1 binding model. However, in the presence of an excess of F^- anion, a remarkable cathodic shift ($\Delta E_{1/2} = -340$ mV) of the oxidation potential is observed. Receptor **1** also showed a perturbation of the oxidation peak in the presence of $\text{HP}_2\text{O}_7^{3-}$ anion. Upon

(25) (a) Descalzo, A. B.; Rurack, K.; Weissshof, H.; Martinez-Mañez, R. M.; Marcos, M. D.; Amorós, P.; Hoffmann, K.; Soto, J. *J. Am. Chem. Soc.* **2005**, *127*, 184–200. (b) Vazquez, M.; Fabbriizzi, L.; Taglietti, A.; Pedrido, R. M.; Gonzalez-Noya, A. M.; Bermejo, M. R. *Angew. Chem., Int. Ed.* **2004**, *43*, 1962–1965. (c) Boiocchi, M.; Dal Boca, L.; Esteban-Gomez, D.; Fabbriizzi, L.; Licchelli, M.; Monzani, E. *J. Am. Chem. Soc.* **2004**, *126*, 16507–16514. (d) Esteban-Gomez, D.; Fabbriizzi, L.; Licchelli, M.; Monzani, E. *Org. Biomol. Chem.* **2005**, *3*, 1495–1500. (e) Evans, L. S.; Gale, P. A.; Light, M. E.; Quesada, R. *Chem. Commun.* **2006**, 965–967. (f) Camiolo, S.; Gale, P. A.; Hursthouse, M. B.; Light, M. E. *Org. Biomol. Chem.* **2003**, *1*, 741–744. (g) Camiolo, S.; Gale, P. A.; Hursthouse, M. B.; Light, M. E.; Shi, A. *J. Chem. Commun.* **2002**, 758–759. (h) Gale, P. A.; Navakhun, K.; Camiolo, S.; Light, M. E.; Hursthouse, M. B. *J. Am. Chem. Soc.* **2002**, *124*, 11228–11229. (i) He, X.; Hu, S.; Liu, K.; Guo, Y.; Xu, J.; Shao, S. *Org. Lett.* **2006**, *8*, 333–336. (j) Viruthachalam, T.; Ramamurthy, P.; Thirumalai, D.; Ramakrishnan, V. *Org. Lett.* **2005**, *7*, 657–660. (k) Caltaginore, C.; Bate, G. W.; Gale, P. A.; Light, M. E. *Chem. Commun.* **2008**, 61–63.

(26) (a) Boiocchi, M.; Del Boca, L.; Esteban-Gomez, D.; Fabbriizzi, L.; Licchelli, M.; Monzani, E. *Chem.–Eur. J.* **2005**, *11*, 3097–3104. (b) Amendola, V.; Boiocchi, M.; Fabbriizzi, L.; Palchatti, A. *Chem.–Eur. J.* **2005**, *11*, 5648–5660. (c) Esteban-Gomez, D.; Fabbriizzi, L.; Licchelli, M.; Sacchi, D. *J. Mater. Chem.* **2005**, *15*, 2670–2675. (d) Esteban-Gomez, D.; Fabbriizzi, L.; Licchelli, M. *J. Org. Chem.* **2005**, *70*, 5717–5720. (e) Ros-Lis, J. V.; Martinez-Mañez, R.; Sancenón, F.; Soto, J.; Rurack, K.; Weissshof, H. *Eur. J. Org. Chem.* **2007**, 2449–2458. (f) Lin, C.; Simov, V.; Drucekhammer, D. G. *J. Org. Chem.* **2007**, *72*, 1742–1746.

(27) Perez-Casas, C.; Yatsimirsky, A. K. *J. Org. Chem.* **2008**, *73*, 2275–2284.

(28) (a) Cho, E. J.; Moon, J. W.; Ko, S. W.; Lee, J. Y.; Kim, S. K.; Yoon, J.; Nam, K. C. *J. Am. Chem. Soc.* **2002**, *125*, 12376–12377. (b) Guunlaugsson, T.; Kruger, P. E.; Lee, T. C.; Parkesh, R.; Pfeffer, F. M.; Hussey, G. M. *Tetrahedron Lett.* **2003**, *44*, 6575–6578. (c) Kubo, Y.; Yamamoto, M.; Ikeda, M.; Takeuchi, M.; Shinkai, S.; Yamaguchi, S.; Tomao, K. *Angew. Chem., Int. Ed.* **2003**, *42*, 2036–2040. (d) Otón, F.; Tárraga, A.; Velasco, M. D.; Espinosa, A.; Molina, P. *Chem. Commun.* **2004**, 1658–1659. (e) Zhang, B.-G.; Xu, J.; Zhao, Y.-G.; Duan, C.-Y.; Cao, X.; Meng, Q.-J. *Dalton Trans.* **2006**, 1271–1276. (f) Otón, F.; Tárraga, A.; Espinosa, A.; Velasco, M. D.; Molina, P. *J. Org. Chem.* **2006**, *71*, 4590–4598. (g) Jang, Y. J.; Jun, E. J.; Lee, Y. J.; Kim, Y. S.; Kim, J. S.; Yoon, J. *J. Org. Chem.* **2005**, *70*, 9603–9606.

(29) Steck, E. A.; Day, A. R. *J. Am. Chem. Soc.* **1943**, *65*, 452–456.

(30) Kaifer, A. E.; Gómez-Kaifer, M. *Supramolecular Electrochemistry*; Wiley-VCH: Weinheim, 1999. (b) Bard, A. J.; Faulkner, L. R. *Electrochemical Methods*, 2nd ed.; Wiley: New York, 2001.

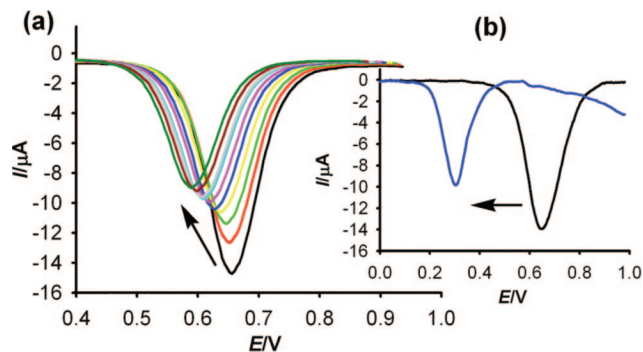


FIGURE 1. Changes in redox properties of **1** (1 mM) in CH_3CN : (a) upon addition of increasing amounts of F^- up to 1 equiv ($c = 2.5 \times 10^{-2}$ M, in CH_3CN) (black); (b) receptor **1** (black) upon addition of 3 equiv of $\text{HP}_2\text{O}_7^{3-}$ ($c = 2.5 \times 10^{-2}$ M, in CH_3CN) (blue).

addition of small amounts of this anion, a new oxidation peak cathodically shifted at 0.30 V ($\Delta E_{1/2} = -340$ mV), appeared. The current intensity of the new oxidation peak increases with a linear dependence on the equiv of the added anion. In particular, this large cathodically shifted oxidation peak reaches the maximum current intensity value at 3 equiv of anion added, and at this point the peak at 0.64 V disappears (Figure 1b). Titration with the strong base Bu_4NOH , which definitely leads to deprotonation, also induced a remarkable cathodic shift of the oxidation peak ($\Delta E_{1/2} = -335$ mV). A possible way to reveal the formation of hydrogen-bonded complexes under conditions of electrochemical titration is to suppress deprotonation by adding a small amount of acetic acid. In preliminary experiments, we found that addition of up to 20 equiv of acetic acid did not affect neither CV nor OSWV of receptor **1** in CH_3CN . Addition of $\text{HP}_2\text{O}_7^{3-}$ anion to an electrochemical solution of receptor **1** in CH_3CN in the presence of 20 equiv of AcOH induced a cathodic shift of the oxidation peak ($\Delta E_{1/2} = -110$ mV) considerably smaller than observed in the absence of acid ($\Delta E_{1/2} = -340$ mV), whereas the addition of F^- anion induces the same change in the oxidation peak that the observed with 1 equiv of added F^- anion ($\Delta E_{1/2} = -70$ mV).

Remarkably, the presence of Cl^- , Br^- , AcO^- , NO_3^- , HSO_4^- , and H_2PO_4^- anions had no effect on the OSWV, even when present in large excess.

In this context, the electrochemical sensing of ATP and ADP by the receptor **1** in MeOH was also studied. At first, titration with Bu_4NOH , indeed, induced a remarkable cathodic shift of the oxidation peak ($\Delta E_{1/2} = -200$ mV). Upon addition of 1 equiv of aqueous ATP or ADP ($c = 2.5 \times 10^{-2}$ M), a new oxidation peak cathodically shifted at 0.57 and 0.60 V ($\Delta E_{1/2} = -70$ and -40 mV) appeared respectively. Under these conditions the $\text{HP}_2\text{O}_7^{3-}$ anion induced a cathodic shift of the oxidation peak higher ($\Delta E_{1/2} = -130$ mV) than those observed for ATP and ADP, but smaller than the found for Bu_4NOH (Figure 2). Results of titration carried out in the presence of 20 equiv of AcOH , indeed show smaller but significant oxidation potential shifts, being remarkable for $\text{HP}_2\text{O}_7^{3-}$ anion ($\Delta E_{1/2} = -56$ mV), and slightly shifted for ADP ($\Delta E_{1/2} = -36$ mV) and ATP ($\Delta E_{1/2} = -40$ mV).

With regard to receptor **2**, addition of Cl^- anions to a solution of this receptor in CH_3CN induced an anodic shift by 80 mV of the reversible oxidation peak ($E_{1/2} = 0.59$ V) due to the Fe(II)/Fe(III) redox process, whereas the irreversible oxidation peaks associated to the Ru center were apparently not perturbed (Figure 3). Remarkably, the presence of Br^- , AcO^- , NO_3^- , HSO_4^- ,

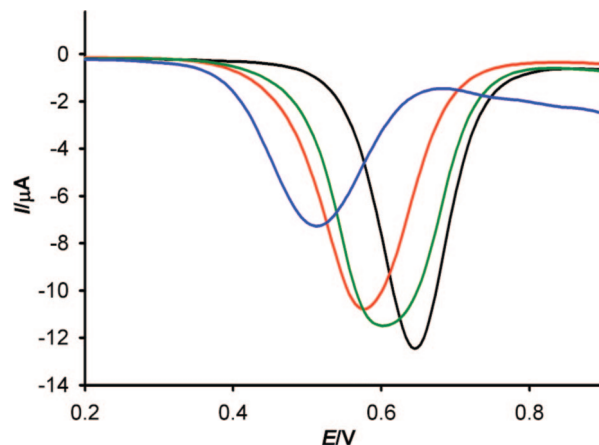


FIGURE 2. Changes in redox properties of **1** (1 mM) in CH_3OH (black) upon addition of 1 equiv of: ADP ($c = 2.5 \times 10^{-2}$ M, in H_2O) (green), ATP ($c = 2.5 \times 10^{-2}$ M, in H_2O) (red), and $\text{HP}_2\text{O}_7^{3-}$ ($c = 2.5 \times 10^{-2}$ M, in H_2O) (blue).

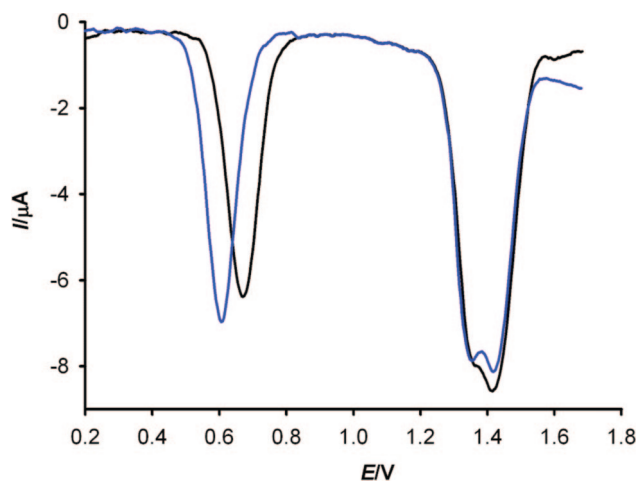


FIGURE 3. Changes in redox properties of **2** (1 mM, in CH_3CN) (black) upon addition of 1 equiv of Cl^- ($c = 2.5 \times 10^{-2}$ M in CH_3CN) (blue).

$\text{HP}_2\text{O}_7^{3-}$, and H_2PO_4^- anions, ATP and ADP had no effect on the OSWV, even when present in large excess. The OSWV of receptor **2** remains unchanged both in the presence of acid (AcOH) or base (Bu_4NOH). The negative shifts in potential result from each anion pushing electron density on to the ferrocene center, making either the complexes or deprotonated species easier to oxidize than their free forms. These electrochemical data show for the first time that the voltammetric techniques are able not only to study anion-receptor interactions but also to discriminate between deprotonation and simple association. The electrochemical data suggest that the interactions between the receptor **1** with ATP and ADP and receptor **2** with Cl^- anion mainly involve hydrogen-bonded complex formation, whereas the interactions of receptor **1** with $\text{HP}_2\text{O}_7^{3-}$ anions involve both formation of hydrogen-bonded complex and deprotonation. Interestingly, the oxidation potential found with or without added acid for the receptor **1** in the presence of 1 equiv of F^- anion could be due to the complex $\mathbf{1}\cdot\text{F}^-$, which in the presence of an excess of anion undergoes deprotonation ($\Delta E_{1/2} = -340$ mV).

The anion binding and sensing properties of receptor **1** and **2** have also been studied by using UV/vis spectroscopic techniques. The UV-vis spectrum of receptor **1** in CH_3CN (c

$= 1 \times 10^{-4}$ M) exhibits strong absorption bands at $\lambda = 256$ nm ($\epsilon = 28\,860$ M $^{-1}$ cm $^{-1}$) and 279 nm ($\epsilon = 31\,780$ M $^{-1}$ cm $^{-1}$), which are tentatively assigned as intraligand (IL) $\pi-\pi^*$ transitions of the 1,10-phenanthroline moiety. Careful evaluation of titration experiments carried out by using the above-mentioned set of aqueous anions ($c = 2.5 \times 10^{-2}$ M) showed that only HP $_2$ O $_7^{3-}$, ATP, and ADP promote remarkable spectral changes. Thus, upon addition of small amounts of HP $_2$ O $_7^{3-}$ anion the two energy bands are red-shifted by 13 and 12 nm respectively and, at the same time, a new strong band at 319 nm ($\epsilon = 28\,300$ M $^{-1}$ cm $^{-1}$) continuously increases in intensity, reaching a maximum when 1 equiv of this anion was added, with the effect that the solution instantaneously changed color from yellow to orange. Isosbestic points at $\lambda = 263$, 272, 285, and 296 nm are found (Figure 4a). The resulting titration isotherm³¹ fits nicely to a 1:1 binding model. Different changes were observed when 1 equiv of ATP or ADP were added: the band at 256 nm remarkably increases in intensity ($\epsilon = 102\,000$ M $^{-1}$ cm $^{-1}$), disappearance of the band at 279 nm and growing of a shoulder peak at 314 nm ($\epsilon = 28\,800$ M $^{-1}$ cm $^{-1}$), with a color change from yellow to pink (Figure 4b). Receptor **1** did not show any obvious spectral change upon addition of either F $^-$, H $_2$ PO $_4^-$ anions or 20 equiv of AcOH. Absorption spectrum of **1** in the presence of Bu $_4$ NOH, however, displayed the same changes that those observed with HP $_2$ O $_7^{3-}$ anions. The spectral profile with HP $_2$ O $_7^{3-}$ anions proceeds with rather approximate isosbestic points in the range 260–290 nm, whereas with Bu $_4$ NOH a clearly additional isosbestic point at 305 nm is observed. This could indicate that the deprotonation by HP $_2$ O $_7^{3-}$ anions is incomplete and the interaction may involve an additional hydrogen-bonded complex. When the spectral evolution of receptor **1** with HP $_2$ O $_7^{3-}$ anions was performed in the presence of added 20 equiv of AcOH, the spectral course of the addition corresponded to those expected for the formation of a hydrogen-bonded complex. The two absorption bands of the receptor appear at the same position and a red-shifted strong absorption band at 287 nm ($\epsilon = 31\,000$ M $^{-1}$ cm $^{-1}$) continuously increasing in intensity indicative of the hydrogen-bonded complex formation, whereas the band at 320 nm due to the deprotonated form was silent (Figure 4c). A well-defined isosbestic point at λ 286 nm, indicative of the presence of only two absorbing species in the solution, is found. To get more information of the interaction of receptor **1** with ADP and ATP, stepwise addition of the anions were performed in the presence of added 20 equiv of AcOH, which suppress completely the deprotonation process, to evaluate the hydrogen-bonded formation. In both cases, the titration profiles were identical to those obtained without acid, these facts clearly indicate that the interaction between the receptor **1** and ADP and ATP involves the formation of an hydrogen-bonded complex.

Assessments of the anion affinities also came from observing the extent to which the fluorescence intensity of **1** and **2** were affected in the presence of anions. Receptor **1** exhibits a very weak fluorescence in CH $_3$ CN ($c = 2.5 \times 10^{-5}$ M) when excited at $\lambda_{\text{exc}} = 390$ nm. The emission spectrum shows a structureless band at 453 nm typical of the imidazophenanthroline ring, with rather low quantum yield ($\Phi = 0.0007$).³² Upon addition of

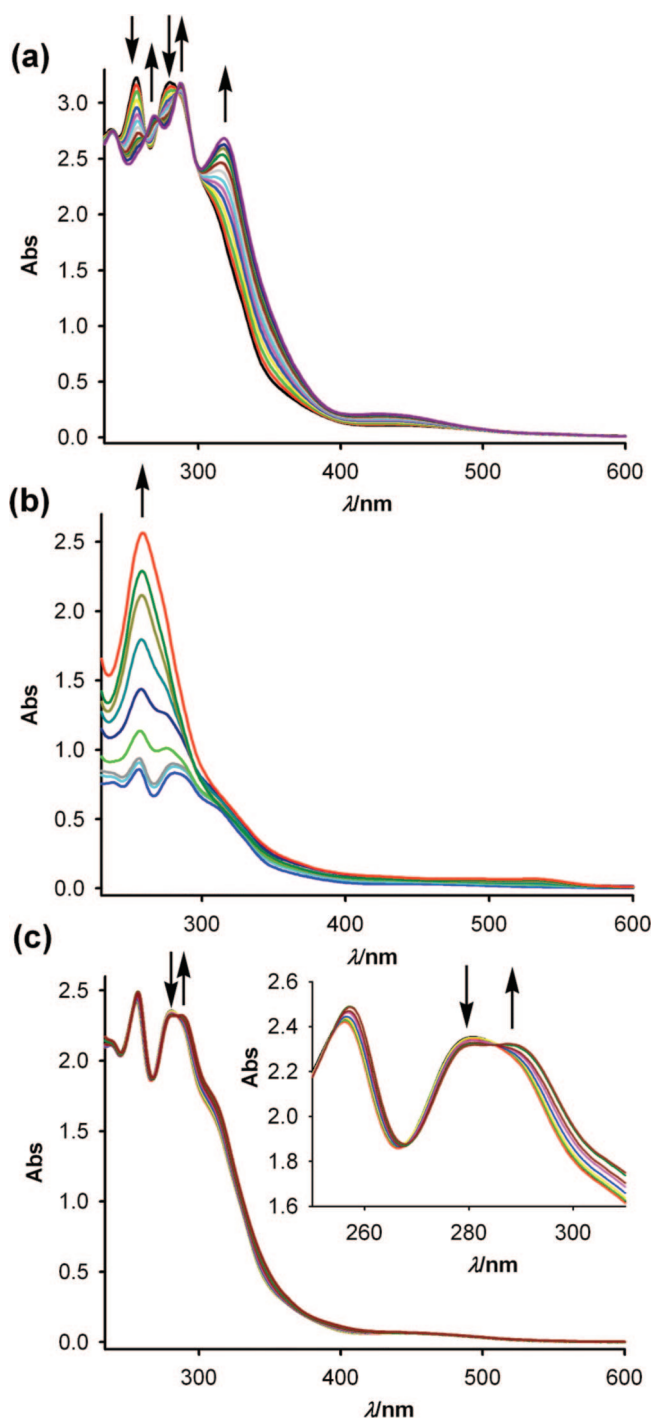


FIGURE 4. (a) Changes in the absorption spectra of **1** (0.1 mM, in CH $_3$ CN) upon addition of increasing amounts of HP $_2$ O $_7^{3-}$ ($c = 2.5 \times 10^{-2}$ M in H $_2$ O). (b) Changes in the absorption spectra of **1** (25 μ M) in CH $_3$ CN upon addition of increasing amounts of ATP ($c = 2.5 \times 10^{-2}$ M in H $_2$ O). (c) Changes in the absorption spectra of **1** (0.1 mM, in CH $_3$ CN) in the presence of 20 equiv of AcOH, upon addition of increasing amounts of HP $_2$ O $_7^{3-}$ ($c = 2.5 \times 10^{-2}$ M in H $_2$ O).

the above-mentioned anions as TBA $^+$ salts in a 2.5-fold excess, no change in the emission spectrum could be observed for Cl $^-$, AcO $^-$, NO $_3^-$, HSO $_4^-$. However, the emission band underwent an important chelation-enhanced fluorescence (CHEF = 50) in the presence of HP $_2$ O $_7^{3-}$ anion, and the quantum yield ($\Phi = 0.022$) resulted in a 31-fold increase compared to that of the receptor **1**. However, a dramatic increase of the emission band

(31) All titrations experiments were analyzed using the computer program Specfit/32 Global Analysis System, 1999–2004, Spectrum Software Associates (SpecSoft@compuserve.com).

(32) The fluorescence quantum yields were measured with respect to anthracene as standard ($\Phi = 0.27$). Dawson, W. R.; Windsor, M. W. *J. Phys. Chem.* **1968**, *72*, 3251–3260.

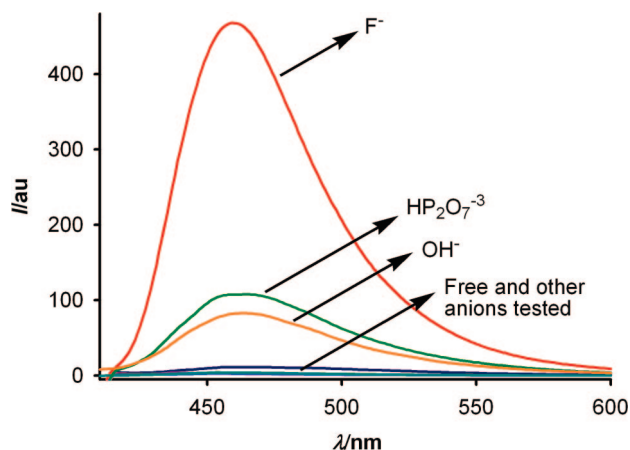


FIGURE 5. Fluorescence spectra of **1** (25 μM , in CH_3CN) in the presence of 25 equiv of several anions ($c = 1 \times 10^{-2}$ M, in H_2O) at $\lambda_{\text{exc}} = 390$ nm.

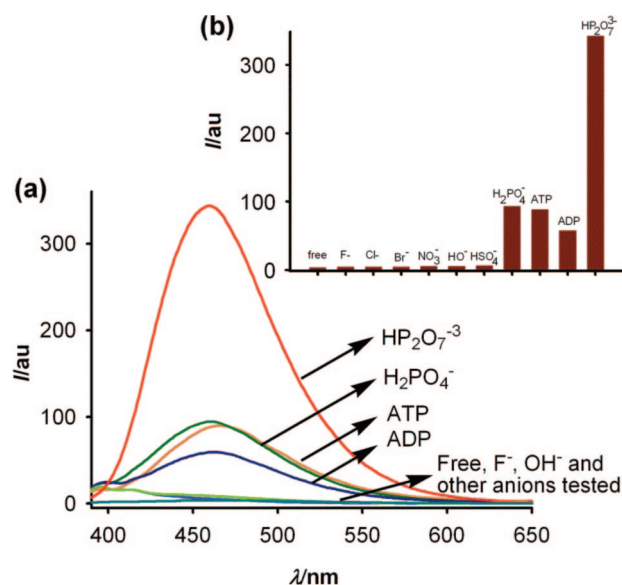


FIGURE 6. (a) Fluorescence spectra of **1** (25 μM) in CH_3CN in the presence of 3 equiv of several anions ($c = 1 \times 10^{-2}$ M in H_2O) at $\lambda_{\text{exc}} = 340$ nm. (b) Fluorescence intensity increase of ligand **1**, in CH_3CN , in relation to the free ligand, after addition of 3 equiv of several anions. Emission is monitored at $\lambda_{\text{exc}} = 340$ nm.

(CHEF = 170) was obtained in the presence of an excess of F^- anion (25 equiv), and the quantum yield ($\Phi = 0.08$) resulted in 114-fold compared to that of receptor **1**. As was expected, addition of 2.5 equiv of Bu_4NOH to a solution of the receptor **1** in CH_3CN also induced an increase of the emission band (CHEF = 34). Interestingly, no change in the emission spectrum was observed after addition of 25 equiv of Cl^- , AcO^- , NO_3^- , HSO_4^- , and H_2PO_4^- anions (Figure 5).

When the previous tested anions, but also including ADP and ATP, were added in aqueous solution ($c = 2.5 \times 10^{-5}$ M) the emission band was also increased with a higher value of the chelation-enhanced fluorescence (CHEF = 60) for $\text{HP}_2\text{O}_7^{3-}$ anion, and the quantum yield ($\Phi = 0.018$) resulted in a 25-fold increased, even though there was a relatively small response (CHEF = 6) with H_2PO_4^- anions (Figure 6).

Interestingly, the dual deprotonation/hydrogen-bonded complex formation behavior of the receptor **1** toward the tested anions could be monitored by carefully selecting the excitation

wavelength. Thus, the emission spectrum of **1** when excited at $\lambda_{\text{exc}} = 340$ nm (Figure 6) displays two very weak and almost overlapped bands at 393 and 413 nm at the same intensity, with a low quantum yield ($\Phi = 0.002$). When aqueous $\text{HP}_2\text{O}_7^{3-}$ anion was added to a CH_3CN solution of **1**, the fluorescent emission spectrum shifted in a dose-dependent manner toward longer wavelengths ($\lambda_{\text{emission}} = 466$ nm). An increase in the $\text{HP}_2\text{O}_7^{3-}$ concentration up to 3 equiv resulted in a 15-fold fluorescence enhancement. The spectral evolution, however, carried out in the presence of added 20 equiv of AcOH displayed a remarkable chelation-enhanced fluorescence (CHEF = 71) and the quantum yield ($\Phi = 0.048$), resulted in a 27-fold increase compared to that of the receptor **1** under these conditions ($\Phi = 0.002$). Taking into account that under these conditions only the hydrogen-bonded complex formation has taken place, the Job plot for the binding between receptor **1** and $\text{HP}_2\text{O}_7^{3-}$ anion show a 1:1 stoichiometry. From the fluorescence titration, the apparent association constant and detection limit³³ were observed to be $6.2 \times 10^4 \text{ M}^{-1}$ and $5.18 \times 10^{-6} \text{ M}^{-1}$. The apparent K_a has been calculated at different concentrations from 1×10^{-4} to 5×10^{-5} M and the found values 5.8×10^4 ($c = 1 \times 10^{-4}$); 6.3×10^4 ($c = 1 \times 10^{-5}$); 6.2×10^4 ($c = 2.5 \times 10^{-5}$); 5.9×10^4 ($c = 5 \times 10^{-5}$), indicate that the apparent association constant of the complex [**1**· $\text{HP}_2\text{O}_7^{3-}$] is independent of the initial concentration of the receptor.

It is important to note that the fluorescent response ($\lambda_{\text{exc}} = 340$ nm) of the receptor **1** toward the anions H_2PO_4^- , ATP, and ADP did no change by the presence or absence of added AcOH . Thus, the addition of 3 equiv of ATP showed a CHEF = 25 accompanied by a 53 nm red-shift of the emission band ($\lambda_{\text{emission}} = 406$ nm). In the presence of H_2PO_4^- anion and ADP, the emission band was also red-shifted by 47 nm ($\lambda_{\text{emission}} = 460$ nm), with CHEF values of 25 for H_2PO_4^- anion 15 for ADP. Quantum yields of the complexes of receptor **1** with the anions H_2PO_4^- , ATP, and ADP are 0.013, 0.012, and 0.008, respectively. The Job plots for the binding between receptor **1** and the three above-mentioned anions show a 1:1 stoichiometry. From the fluorescence titration, the apparent association constants and detection limits were observed to be 5.1×10^4 and 2.1×10^{-5} M (H_2PO_4^-), 4.5×10^5 and 1.8×10^{-5} M (ATP), and 1.4×10^4 and 1.5×10^{-5} M (ADP), respectively.

Several trends have surfaced from the spectral emission data. First, the emission band associated to $\lambda_{\text{exc}} = 390$ nm could be due to the deprotonated form, whereas the band associated at $\lambda_{\text{exc}} = 340$ nm probably is due to the hydrogen-bonded formation. Second, suppression of the deprotonation process by adding excess of AcOH , allow to monitor only the formation of hydrogen-bonded complexes. Third, with F^- anions only the deprotonation process is observed, by contrast with H_2PO_4^- , ATP, and ADP only the formation of hydrogen-bonded complexes is achieved. Fourth, emission bands are observed when a solution of the receptor **1** in the presence of $\text{HP}_2\text{O}_7^{3-}$ anion was excited either at 340 nm (hydrogen-bonded complex formation) or 390 nm (deprotonation); thus, we conclude that the formation of hydrogen-bonded complex between receptor **1** and $\text{HP}_2\text{O}_7^{3-}$ anion and deprotonation proceed simultaneously.

We examined the reversibility of anion sensing. If the sensing system is reversible, depletion of the anion that coordinates **1** must produce a change of either the absorption or emission spectrum, causing it to revert to the original spectrum. An excess

(33) Shortreed, M.; Kopelman, R.; Kuhn, M.; Hoyland, B. *Anal. Chem.* **1996**, *68*, 1414–1418.

amount of Mg^{2+} was added to this $[\mathbf{1}\cdot\text{HP}_2\text{O}_7^{3-}]$ solution (formed by adding 1 equiv $\text{HP}_2\text{O}_7^{3-}$ anion to a solution of receptor $\mathbf{1}$ and 20 equiv of AcOH) to bind $\text{HP}_2\text{O}_7^{3-}$ and prevent $\text{HP}_2\text{O}_7^{3-}$ from coordinating $\mathbf{1}$. When 1 equiv of $\text{Mg}(\text{ClO}_4)_2$ was added to a solution of $[\mathbf{1}\cdot\text{HP}_2\text{O}_7^{3-}]$, the absorption and emission spectra almost exactly coincided with the spectrum of $\mathbf{1}$ containing no $\text{HP}_2\text{O}_7^{3-}$. Formation of the complex $[\mathbf{1}\cdot\text{HP}_2\text{O}_7^{3-}]$ and the subsequent trapping of the anion were carried out over several cycles. The optical and emission spectra were recorded after each step and were found to be fully recovered on completion of the step, thus demonstrating the high degree of reversibility of the sensing process.

The UV-vis spectrum of receptor $\mathbf{2}$ in CH_3CN ($c = 2.5 \times 10^{-4}$ M) displays two strong high energy bands at $\lambda = 250$ nm ($\epsilon = 41\,460$ $\text{M}^{-1}\text{cm}^{-1}$) and 267 nm ($\epsilon = 47\,010$ $\text{M}^{-1}\text{cm}^{-1}$) due to intraligand (IL) $\pi-\pi^*$ transitions, and a weak low energy band located at $\lambda = 457$ nm ($\epsilon = 17\,920$ $\text{M}^{-1}\text{cm}^{-1}$), assigned to metal-to-ligand charge transfer (MLCT) transitions.³⁴ The emission spectrum obtained by excitation at 260 nm exhibits a very weak band at $\lambda = 612$ nm, which is characteristic of ³MLCT luminescence [$d\pi(\text{Ru})-\pi^*(\text{ligand})$], with a rather low quantum yield ($\Phi = 0.0007$). No changes were observed in the absorption spectrum of $\mathbf{2}$ upon anion recognition, only addition of 1 equiv of Bu_4NOH induces a red-shift of the two high energy bands by 85 and 163 nm respectively, growing of a shoulder peak at 532 nm along with the initial low energy band at 459 nm. The changes in the emission spectrum of $\mathbf{2}$ were examined when screened with the 10 above-mentioned anions. Remarkably, only Cl^- anion caused a dramatic change in the emission spectrum of $\mathbf{2}$. The addition of 1 equiv of Cl^- anion increases the integrated fluorescence intensity in a 30-fold and the quantum yield ($\Phi = 0.003$) resulted in a 43-fold increase (Figure 7). The stoichiometry of the complex system was also determined by the changes in the fluorogenic response of $\mathbf{2}$ in the presence of varying concentrations of Cl^- , and the results obtained indicated the formation of a 1:1 complex giving an association constant of 4.5×10^4 M^{-1} and a detection limit of 2×10^{-5} M.

Due to its spherical structure and relative large ionic radius, Cl^- anion recognition is not trivial and often requires the use of structurally complex hosts.³⁵ A few examples have recently been reported demonstrating the feasibility of the use of small and hence structurally simple molecules for such recognition.³⁶

The stoichiometry of the complexes have also been confirmed by ESI-MS, where peaks at m/z 581 $[\mathbf{1}\cdot\text{HP}_2\text{O}_7^{3-}]$, m/z 957 $[\mathbf{1}\cdot\text{ATP}]$, and m/z 1142 $[\mathbf{2}\cdot\text{Cl}^-]$ are observed. The relative abundance of the isotopic clusters was in good agreement with the simulated spectra of the 1:1 complexes (Figure 8).

To look into the anion binding properties of receptors $\mathbf{1}$ and $\mathbf{2}$ ¹H NMR experiments were carried out both in the absence

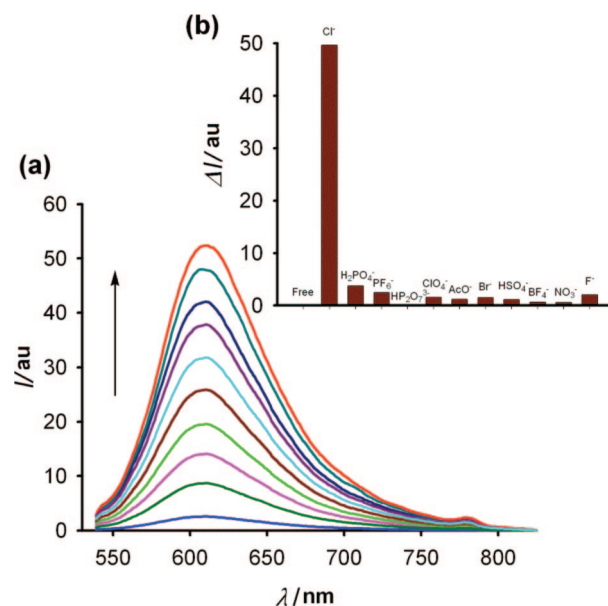


FIGURE 7. (a) Changes in the fluorescence emission spectrum of $\mathbf{2}$ ($c = 2.5 \times 10^{-5}$ M in CH_3CN) upon titration with Cl^- : the initial (blue) is that of $\mathbf{2}$ and the final one (red), after addition of 1 equiv of Cl^- . (b) Fluorescence intensity increase of ligand $\mathbf{2}$, in CH_3CN , in relation to the free ligand, after addition of 1 equiv of several anions. Emission is monitored at $\lambda_{\text{exc}} = 260$ nm.

and presence of anions in acetonitrile- d_3 or methanol- d_4 at room temperature. It must be considered that hydrogen bond formation between the receptors and the anions can induced two distinct effects on the heteroaromatic and metallocene protons: (a) it increases the electron density of the both units with a through-bond propagation, which generates a shielding effect and should produce an upfield shift of the C-H protons; and (b) it induces the polarization of the C-H bonds via a through space effect, which causes a deshielding effect and produces a downfield shift. The latter effect, of electrostatic nature drastically decreases upon increasing the distance between the envisaged C-H proton and the site of H-bond interaction.

When one equiv of TBAF was added to a solution of $\mathbf{1}$ in acetonitrile- d_3 its ¹H NMR spectrum displayed dramatic changes (Figure 9). The N-H proton, which in the free receptor appears at δ 11.3 ppm, disappeared and a clear upfield shift for 3-H ($\Delta\delta = -0.13$ ppm) and 2-H ($\Delta\delta = -0.18$ ppm) was observed. On the contrary, the signal for 4-H was shifted downfield ($\Delta\delta = +0.25$ ppm). Meanwhile, upfield shifts of the signals corresponding to the unsubstituted cyclopentadienyl ring ($\Delta\delta = -0.15$ ppm) and to the β protons of the monosubstituted cyclopentadienyl ring ($\Delta\delta = -0.28$ ppm) were also observed. Moreover, the α protons were downfield shifted ($\Delta\delta = +0.17$ ppm). The electrostatic effect predominates for the heteroaromatic 4-H proton and the α -protons of the monosubstituted cyclopentadienyl ring as indicated by the pronounced downfield shift. Heteroaromatic protons 2-H and 3-H are too far away from the N-H protons to be subjected to any electrostatic effect. Thus, the shielding effect induced by the propagation of electron density is not contrasted and a significant upfield shift is observed. It may be surprising that the unsubstituted cyclopentadienyl ring protons, quite far away from the N-H fragment, undergo substantial downfield shift.

Likewise, addition of 2.5 equiv of $\text{HP}_2\text{O}_7^{3-}$ anion caused similar chemical shift changes, although now well-resolved signals for the aromatic protons were obtained (Figure 9). In

(34) (a) Juris, A.; Balzani, V.; Barigelletti, F.; Campagna, S.; Belsler, P.; Zelewsky, A. V. *Coord. Chem. Rev.* **1988**, *84*, 85–277. (b) Beer, P. D.; Szemes, F.; Balzani, V.; Salá, C. M.; Drew, M. G. B.; Dent, S. W.; Maestri, M. *J. Am. Chem. Soc.* **1997**, *119*, 11864–11875. (c) Anzenbacher, P., Jr.; Tyson, D. S.; Jursikova, K.; Castellano, F. N. *J. Am. Chem. Soc.* **2002**, *124*, 6232–6233.

(35) (a) Davis, A. P.; Joos, J. B. *Coord. Chem. Rev.* **2003**, *240*, 143–156. (b) Boon, J. M.; Smith, B. D. *Curr. Opin. Chem. Biol.* **2002**, *6*, 749–756. (c) McNally, B. A.; Koulou, A. V.; Smith, B. D.; Joos, J. B.; Davis, A. P. *Chem. Commun.* **2005**, 1087–1089.

(36) (a) Zhang, Y.; Li, M. X.; Lü, M. Y.; Yang, R. H.; Liu, F.; Li, K. A. *J. Phys. Chem. A* **2005**, *109*, 7442–7448. (b) Bai, Y.; Zhang, B.-G.; Xu, J.; Duan, C.-Y.; Dang, D. B.; Liu, D.-J.; Meng, Q.-J. *New J. Chem.* **2005**, *29*, 777–779. (c) Schazmann, B.; Alhashimi, N.; Diamond, D. *J. Am. Chem. Soc.* **2006**, *128*, 8607–8614. (d) dos Santos, C. M. G.; McCabe, T.; Gunnlaugsson, T. *Tetrahedron Lett.* **2007**, *48*, 3135–3139.

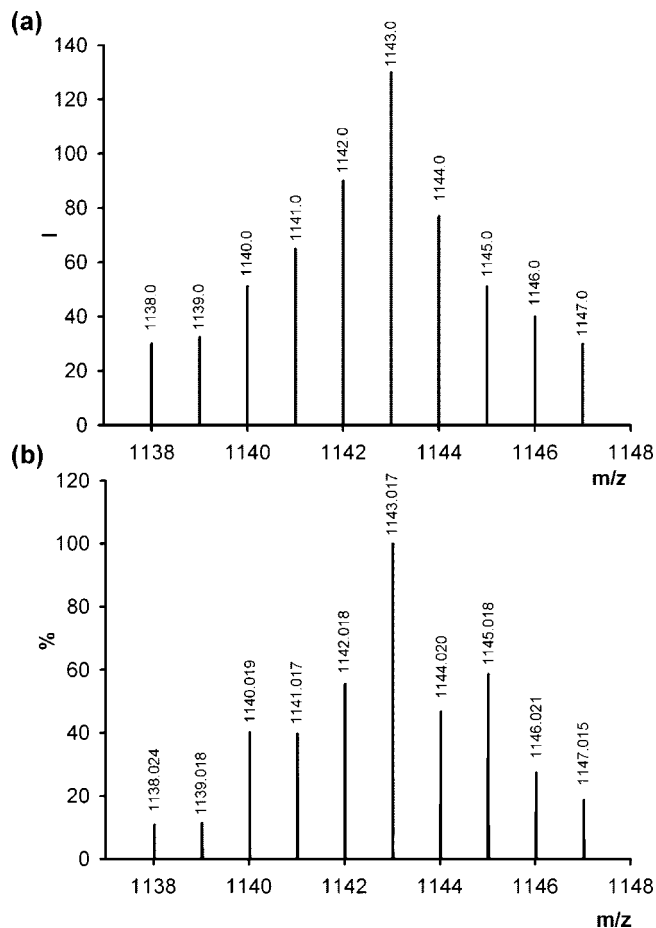


FIGURE 8. Electrospray mass spectrum of a $2 \cdot \text{Cl}^-$ sample, in acetone solution. (Top) Measured pattern of the complex. (Bottom) Calculated pattern of the complex.

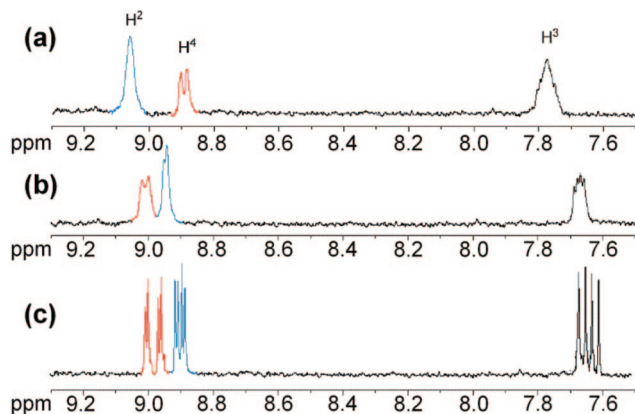


FIGURE 9. ^1H NMR spectral changes observed in the aromatic region of **1**, in acetonitrile- d_3 , after the addition of (a) 0 equiv of anions, (b) 1 equiv of F^- , and (c) 2.5 equiv of $\text{HP}_2\text{O}_7^{3-}$.

methanol- d_4 solution, the N–H proton was silent, and when these titrations were carried out in this deuterated solvent and the anions were added in D_2O solutions the most relevant interaction-induced chemical shift was found to be a downfield shift for the 4-H proton: $\Delta\delta = +0.10$ ppm for $\text{HP}_2\text{O}_7^{3-}$, $+0.23$ ppm for ATP, and $+0.17$ for ADP (Figure 10a). In the spectrum of the receptor **1** after addition of 2 equiv of Bu_4NOH the 4-H protons are also downshifted ($\Delta\delta = +0.10$ ppm), whereas the α -protons of the substituted cyclopentadienyl ring remains almost at the same position. The remaining ferrocene protons

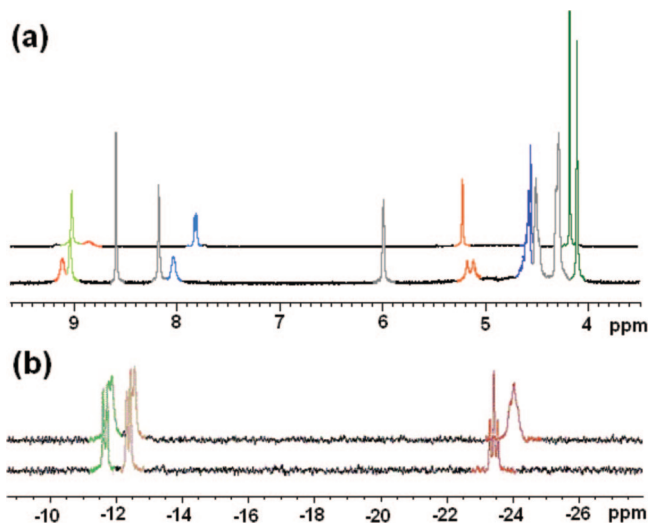


FIGURE 10. (a) ^1H NMR spectral changes observed in **1** (top) in CD_3OD , after the addition of 1 equiv ATP (bottom). (b) ^{31}P NMR spectral changes observed in ATP (top) in CD_3OD , after the addition of 1 equiv of **1** (bottom).

and 2-H and 4-H heteroaromatic protons are upfield shifted as they were with $\text{HP}_2\text{O}_7^{3-}$ anions. Results of the stepwise addition of $\text{HP}_2\text{O}_7^{3-}$ anion to a solution of the receptor **1** in the presence of added 20 equiv of AcOH, show characteristics expected for formation of a hydrogen-bonding complex. Signals for heteroaromatic 4-H and α -cyclopentadienyl protons gradually broadened but are still detectable and show a characteristic for hydrogen-bonding strong downfield shift: $\Delta\delta = +0.24$ ppm for 4-H and $\Delta\delta = +0.28$ ppm for the α -protons, whereas the heteroaromatic 2-H, 3-H, and β -cyclopentadienyl protons remained unchanged. These results suggest that, in addition, to the formation of hydrogen-bonds between the anion and the N–H proton, $\text{HP}_2\text{O}_7^{3-}$ anion interacts strongly with the 4-H of the heteroaromatic ring and the α -protons of the substituted cyclopentadienyl ring of the ferrocene fragment. By contrary, the spectrum of receptor **1** in the presence of added 20 equiv of AcOH after adding excess of F^- anions remained unchanged, which clearly suggests that under these conditions the interaction between them only involves deprotonation.

The ^{31}P NMR spectrum of the receptor **1** in the presence of $\text{HP}_2\text{O}_7^{3-}$ anions showed that the signals due to the two different phosphorus atoms in the hydrogen pyrophosphate anion moved at the same extension, from -4.9 to -7.1 ppm ($\Delta\delta = -2.2$ ppm) and from 3.6 to 1.5 ppm ($\Delta\delta = -2.1$ ppm), respectively, which indicates that receptor **1** directly interacts with the phosphate sites. When the complexation process between the receptor **1** and ATP was evaluated, the signal of the β -phosphate of ATP is higher shifted to the downfield ($\Delta\delta = +0.61$ ppm), than the α - and γ -phosphate ($\Delta\delta = +0.15$ and $+0.23$ ppm) signals respectively,³⁷ which suggest that receptor **1** predominantly binds to the β -phosphate of ATP (Figure 10b). On the other hand, the chemical shifts of the α - and β -phosphate of the ADP scarcely changes in the presence of receptor **1** ($\Delta\delta = +0.02$ ppm).

The ^1H NMR spectrum of the heterobimetallic receptor **2** in acetone- d_6 displays the characteristics signals assigned to this kind of compounds.³⁸ The protons of the imidazophenanthroline

(37) Bock, J. L. *Inorg. Biochem.* **1980**, *12*, 119–130.

(38) Xu, H.; Zheng, K.-C.; Deng, H.; Lin, L.-J.; Zhang, Q.-L.; Ji, L.-N. *New J. Chem.* **2003**, *27*, 1255–1263.

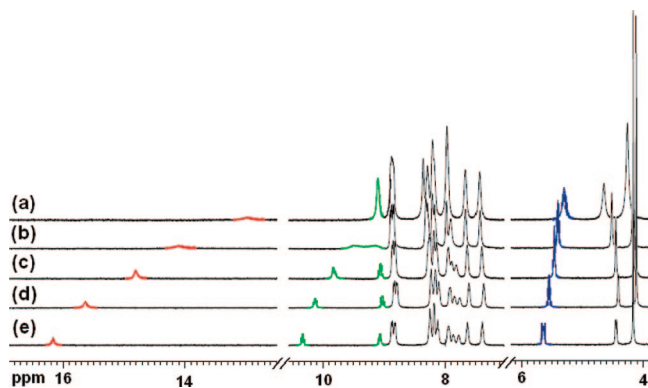


FIGURE 11. ^1H NMR spectral changes observed for **2**, in acetone- d_6 , after addition of increasing amounts of Cl^- in CD_3CN : (a) 0, (b) 0.25, (c) 0.50, (d) 0.75, and (e) 1 equiv.

ring appear as a set of three signals: a doublet centered at 9.07 (4-H), a doublet at 8.20 (2-H) and a triplet at 7.92 (3-H) ppm respectively, whereas the N–H proton appears at $\delta = 13.0$ ppm. Only the Cl^- anion caused a downfield shift of some signals, indicative of an H-bonding interaction. Upon addition of Cl^- anion in the form of TBA salt, the signal of the 4-H protons is splitted into two signals, one of them is shifted to downfield at 10.33 ppm ($\Delta\delta = +1.33$ ppm) and the second one remains at the same position. Meanwhile, downfield shift of the signals corresponding to the α -protons of the monosubstituted cyclopentadienyl ring ($\Delta\delta = +0.43$ ppm) was also observed. A notable feature of this titration is that the resonance corresponding to the imidazole N–H proton is downfield shifted ($\Delta\delta = +3.16$ ppm) over the course of the titration. The fact that this signal is observable throughout the titration is inconsistent with a deprotonation process involving the receptor, and probably the formation of a hydrogen-bonded complex has taken place (Figure 11). This assumption is also supported by the fact that addition of 1 equiv of Bu_4NOH to a solution of the receptor **2** did not induce any significant change.

Accordingly, the spectroscopic data led us to the conclusion that the Cl^- anions had more effective hydrogen bond interactions not only with the N–H proton but also with the aromatic and ferrocenyl protons, which could be another example of N–H based receptor in which C–H hydrogens participate in supplementary hydrogen bonding with anions.³⁹

Theoretical Calculations. Quantum chemical calculations at the DFT level of theory (see the Supporting Information) has allowed satisfactory explanation about binding modes between the receptors and the complexed anions. Under the working conditions, that is using naked anions (no counteraction was explicitly included) in the modelization and optimizations being carried out in the gas-phase, both F^- and $\text{HP}_2\text{O}_7^{3-}$ anions promote deprotonation of the ligand **1**. The obtained structures (Figure 12) are therefore resulting from the complexation of the conjugated acids of the anions HF and $\text{H}_2\text{P}_2\text{O}_7^{3-}$, by the action of the conjugated base of ligand **1** still featuring a concave

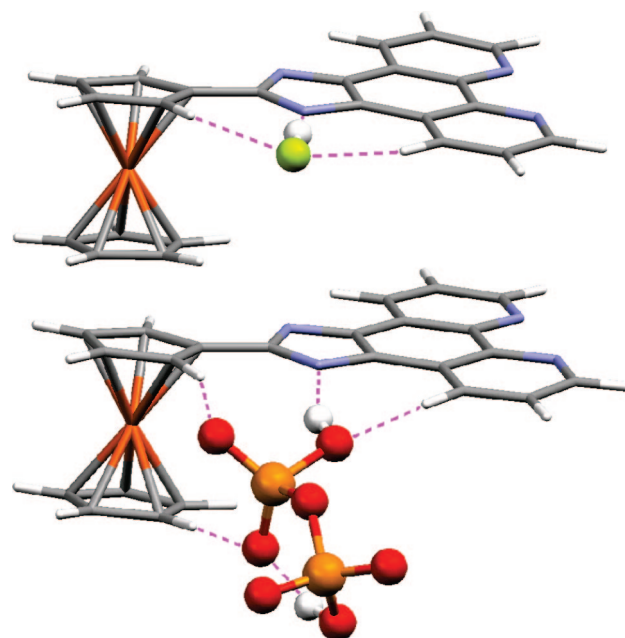


FIGURE 12. Calculated (B3LYP/aug-6-31G*) structures for complexes $\mathbf{1}\cdot\text{F}^-$ (up) and $\mathbf{1}\cdot\text{HP}_2\text{O}_7^{3-}$ (down).

surface with acidic H atoms directed in a convergent fashion. Thus after initial endergonic acid–base proton transfer ($\Delta G_{\text{MeCN}} = +11.28$ Kcal·mol $^{-1}$), complexation of F^- is predicted to be moderately exergonic ($\Delta G_{\text{MeCN}} = -5.44$ Kcal·mol $^{-1}$) and occurs upon little deformation of the free-ligand structure ($L_{\text{strain}} = 1.53$ Kcal·mol $^{-1}$). A partial deprotonation in $\mathbf{1}\cdot\text{F}^-$ is evidenced by the pyrrolic H atom being almost halfway in between nitrogen ($d_{\text{N}\cdots\text{H}} = 1.279$ Å, WBI 0.373) and fluorine ($d_{\text{F}\cdots\text{H}} = 1.150$ Å, WBI 0.378) atoms (angle NHF 178.3°), the later forming in addition two weak hydrogen bridge bonds with phenanthroline 4-H ($d_{\text{F}\cdots\text{4H}} = 2.378$ Å, WBI 0.019) and ferrocenyl H α ($d_{\text{F}\cdots\text{H}\alpha} = 2.378$ Å, WBI 0.017). On the contrary, deprotonation by hydrogenpyrophosphate is expected to be slightly exergonic ($\Delta G_{\text{MeCN}} = -0.53$ Kcal·mol $^{-1}$), although global complexation resulted moderately endergonic ($\Delta G_{\text{MeCN}} = +8.20$ Kcal·mol $^{-1}$), presumably due mainly to highly unfavorable entropic component, higher ligand deformation ($L_{\text{strain}} = 6.10$ Kcal·mol $^{-1}$), and higher relevance of the naked-anion effect in this trianionic substrate. For the calculated structure of $\mathbf{1}\cdot\text{HP}_2\text{O}_7^{3-}$ complex, partial wrapping of one $\text{H}_2\text{P}_2\text{O}_7^{2-}$ phosphate unit by the convergent preorganized cavity of the conjugated base (fully deprotonated) of **1** is observed. One strong hydrogen bridge bond of O–H \cdots N type ($d_{\text{N}\cdots\text{H}} = 1.279$ Å, WBI 0.373; angle OHN 160.0°) and a weaker one between this oxygen atom and the phenanthroline 4-H ($d_{\text{O}\cdots\text{4H}} = 2.297$ Å, WBI 0.010) binds the anion to the imidazophenanthroline part of the receptor, whereas two additional relatively short O \cdots H bonds with H α ($d_{\text{O}\cdots\text{H}\alpha} = 2.235$ Å, WBI 0.020) at Cp $_a$ (the monosubstituted cyclopentadienyl ring) and one H–Cp $_b$ (Cp $_b$ = unsubstituted cyclopentadienyl ring; $d_{\text{O}\cdots\text{HCp}_b} = 2.192$ Å, WBI 0.022) catch hold of the ferrocenyl part, thus hindering rotation around the ferrocene–imidazole bond (see below). Then, we assume that the well-resolved signals observed in the ^1H NMR of $\mathbf{1}\cdot\text{HP}_2\text{O}_7^{3-}$ complex, previously described, could be a consequence of this hindered rotation.

The NBO (Natural Bond Orbital) analysis reveals that the uppermost valence AO (atomic orbitals) at the iron centers in every molecular system are roughly half-populated e_{1g} -type 3d

(39) (a) Tárraga, A.; Molina, P.; López, J. L.; Velasco, M. D.; Bautista, D.; Jones, P. G. *Organometallics* **2002**, *21*, 2055–2065. (b) Lee, C.-H.; Na, H.-K.; Yoon, D.-H.; Cho, W.-S.; Lynch, V. M.; Shevchuck, S. V.; Sessler, J. L. *J. Am. Chem. Soc.* **2003**, *125*, 7301–7306. (c) Kwon, J. Y.; Jang, Y. J.; Kim, S. K.; Lee, K.-H.; Kim, J. S.; Yoon, J. *J. Org. Chem.* **2004**, *69*, 5155–5157. (d) Ghosh, S.; Choudhury, A. R.; Row, T. N. G.; Maitra, U. *Org. Lett.* **2005**, *7*, 1441–1444. (e) Lu, H. L.; Zhang, D.; Chen, C.; Zhu, D. *Org. Lett.* **2005**, *7*, 4629–4632. (f) El Drubi, I.; Gale, P. A.; Light, M. E.; Loeb, S. J. *Chem. Commun.* **2005**, 4913–4915. (g) Xu, Z.; Kim, S.; Lee, K.-H.; Yoon, J. *Tetrahedron Lett.* **2007**, *48*, 3797–3800.

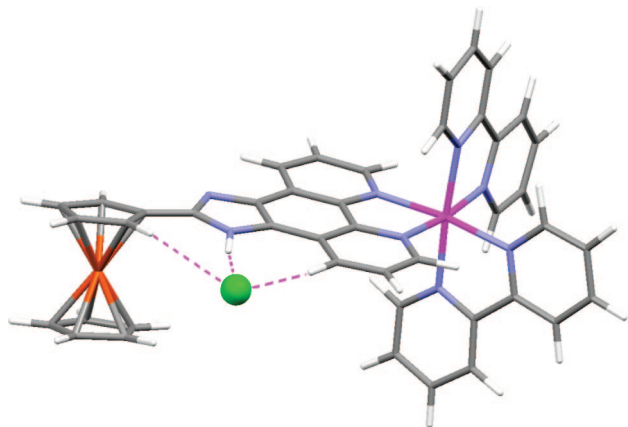


FIGURE 13. Calculated (B3LYP/aug-6-31G*/SDD-ecp) structure for the complex $[1\cdot\text{Ru}(\text{bipy})_2\cdot\text{Cl}]^+$.

TABLE 1. Calculated (GIAO/CPCM/B3LYP/aug-6-311G**//B3LYP/aug-6-31G*) ^1H NMR Chemical Shifts (ppm)^a for Receptor $[1\cdot\text{Ru}(\text{bipy})_2]^{2+}$ and Complex $[1\cdot\text{Ru}(\text{bipy})_2\cdot\text{Cl}]^+$ in Acetone Solution

		$[1\cdot\text{Ru}(\text{bipy})_2]^{2+}$	$[1\cdot\text{Ru}(\text{bipy})_2\cdot\text{Cl}]^+$	
		δ^{H}	δ^{H}	$\Delta\delta^{\text{H}}(\text{exp})$
C _p a	H α	5.25	5.59	0.24 (0.43)
	H β	4.69	4.65	-0.04 (-0.22)
C _p b		4.26	4.18	-0.08 (0.02)
	2-H	8.53	8.38	-0.15 (0.00)
Phenan.	3-H	8.37	8.25	-0.12 (-0.08)
	4-H	9.59	11.85	2.26 (1.23)
N-H			9.68	0.09 (0.01)
		10.47	16.88	6.41 (3.16)

^a Average for related protons.

AO and their energies increase following the degree of deprotonation (see above) in the series 1 (-0.162 au) < $1\cdot\text{F}^-$ (-0.040 au) < $1\cdot\text{HP}_2\text{O}_7^{3-}$ (+0.121 au), in perfect agreement with the increasing ease of oxidation experimentally shown by their lower (cathodically shifted) oxidation potentials.

Also, the structures of $[1\cdot\text{Ru}(\text{bipy})_2]^{2+}$ (see the Supporting Information), that is, 2 without the counteranions, and $[1\cdot\text{Ru}(\text{bipy})_2\cdot\text{Cl}]^+$ (Figure 13) have been calculated. The NBO analysis reveals that the uppermost valence AO at Fe are, in these cases, of a_{1g} symmetry (d_{z^2} type) and also roughly half-populated. As expected, this AO in $[1\cdot\text{Ru}(\text{bipy})_2]^{2+}$ has lower energy content (-0.286 au) than that in 1 , hence its higher (anodically shifted) oxidation potential. Upon complexation of Cl^- , the energy of this AO increases (-0.184 au), which is in agreement with the observed cathodic shift experienced by the corresponding oxidation wave. Complexation of Cl^- occurs upon little deformation of the free-ligand structure ($L_{\text{strain}} = 1.38 \text{ Kcal}\cdot\text{mol}^{-1}$) and is predicted to be only slightly exergonic ($\Delta G_{\text{MeCN}} = -1.10 \text{ Kcal}\cdot\text{mol}^{-1}$). Selectivity toward other spherical halide anions has also been studied. For that purpose, the optimized structures of $[1\cdot\text{Ru}(\text{bipy})_2\cdot\text{F}]^+$ and $[1\cdot\text{Ru}(\text{bipy})_2\cdot\text{Br}]^+$ (see the Supporting Information) were obtained. Complexation of F^- anion takes place with a comparatively remarkable deformation of the ligand ($L_{\text{strain}} = 3.68 \text{ Kcal}\cdot\text{mol}^{-1}$), much higher than that found for $1\cdot\text{F}^-$. Ligand deformation is small upon complexation of Br^- anion ($L_{\text{strain}} = 1.14 \text{ Kcal}\cdot\text{mol}^{-1}$) and, in this case, selectivity may arise from the slightly endergonic character ($\Delta G_{\text{MeCN}} = +0.24 \text{ Kcal}\cdot\text{mol}^{-1}$) of the ligand-anion recognition event. The calculated structure for the $[1\cdot\text{Ru}(\text{bipy})_2\cdot\text{Cl}]^+$ complex is characterized by strong N-H...Cl bridge bonding with the

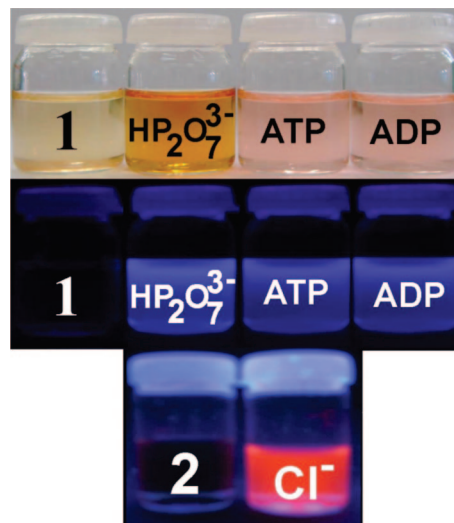


FIGURE 14. Changes in the color of ligand 1 (up) and in the fluorescence of ligands 1 and 2 (down) upon addition of the corresponding anions.

pyrrolic H atom ($d_{\text{Cl}\cdots\text{H}} = 1.963 \text{ \AA}$, WBI 0.181; angle NHCl 169.5°), and the guest Cl^- anion forming a complementary hydrogen bridge bond with phenanthroline 4-H ($d_{\text{Cl}\cdots\text{4H}} = 2.376 \text{ \AA}$, WBI 0.037), as well as two other weak ones with ferrocenyl H α ($d_{\text{Cl}\cdots\text{H}\alpha} = 2.925 \text{ \AA}$, WBI 0.004) and H-C_pb ($d_{\text{Cl}\cdots\text{H-Cp}_b} = 3.155 \text{ \AA}$, WBI 0.002).

The calculated spectra for both the receptor $[1\cdot\text{Ru}(\text{bipy})_2]^{2+}$ and the corresponding complex $[1\cdot\text{Ru}(\text{bipy})_2\cdot\text{Cl}]^+$ (Table 1) fit nicely with those obtained experimentally (see the Supporting Information), which supports the theoretical findings concerning the nature of binding of chloride anions to the receptor. The remarkable downfield shifting of the N-H and phenanthroline 4-H signals constitutes a direct consequence of the hydrogen bridge bonding with the chloride anion guest.

Conclusions

In summary, we describe an easy-to-synthesize ferrocene-based imidazophenanthroline 1 and its stable Ru(II) complex 2 receptors and examined their properties toward various guest anions, using electrochemical, spectral and fluorescence techniques. Receptor 1 in acetonitrile senses aqueous hydrogenpyrophosphate and the organic anions ADP and ATP through three different channels: the yellow-to-orange or pink color change which allow the potential for “naked eye” detection, a red-shift of the emission band with an important fluorescent enhancement, and an unprecedented large cathodic shift of the ferrocene oxidation wave (Figure 14). About the deprotonation/coordination dualism, the combined electrochemical, absorption, emission, and NMR data strongly support that fluoride anion induces only deprotonation, anions, dihydrogenphosphate, ATP, and ADP from hydrogen-bonded complexes and formation of hydrogen-bonded complex between receptor 1 and hydrogenpyrophosphate anion and deprotonation proceed simultaneously. As a consequence, selective fluorescent detection of hydrogenpyrophosphate anions in the presence of the related competitors dihydrogenphosphate anions, ADP, and ATP could be achieved by carefully selection of the excitation energy. The recognition event has also been studied by ^1H and ^{31}P NMR spectroscopy, as well as by DFT calculations.

The use of ruthenium(II) fluorophore in receptor 1 has a large effect on the resulting function, specifically anion binding in

the present instance.⁴⁰ Remarkably, the heterobimetallic receptor **2** exhibits not only a high selectivity for chloride anion over other anions with important fluorescent enhancement but also a special electrochemical recognition with remarkable cathodic shift of the ferrocene oxidation wave. ¹H NMR spectrum of the complex indicates that not only the N–H but also that heteroaromatic and cyclopentadienyl protons participate in an authentic hydrogen-bonded complex. The anion sensing behavior of complex **2** provides a nice example of a switchable fluorescent chemosensor molecule mediated by metal ion coordination.

Experimental Section

2-Ferroceny-1H-imidazo[4,5-f][1,10]-phenanthroline 1. To a solution of 1,10-phenanthroline-5,6-dione (0.250 g, 1.18 mmol) in chloroform (25 mL) were added ammonium acetate (1.18 g, 0.023 mmol), formyl ferrocene (0.254 g, 1.18 mmol), and acetic acid (1 mL). The reaction mixture was stirred and heated at reflux temperature for 12 h. After cooling, the solution was neutralized with a saturated aqueous NaHCO₃ solution and then extracted with chloroform (3 × 25 mL). The combined organic layers were dried on MgSO₄ and filtered, and the filtrate was concentrated to dryness to give a solid residue that was recrystallized from CH₂Cl₂ to give **1** in 98% yield. Mp > 300 °C. ¹H NMR (400 MHz, CD₃CN): δ 4.18 (s, 5H), 4.52 (st, 2H), 5.15 (st, 2H), 7.76 (bs, 2H), 8.89 (d, 2H, *J* = 8.4 Hz), 9.16 (bs, 2H), 11.3 (bs, 1H). ¹³C NMR (100 MHz, CD₃CN): δ 62.1 (CH), 64.3 (CH), 64.6 (CH), 69.8 (q), 117.9 (CH), 124.2 (q), 138.8 (2q), 138.9 (CH), 142.3 (CH), 147.3 (q). MS (70 eV, EI): *m/z* (relative intensity): 404 (100, M⁺), 339 (10), 281 (11), 221 (11), 154 (24), 149 (15), 147 (30), 137 (18), 107 (11). Anal. Calcd for C₂₃H₁₆FeN₄: C, 68.34; H, 3.99; N, 13.86. Found: C, 68.39; H, 4.10; N, 13.77.

Ruthenium (II) (2-Ferrocenyl-1H-imidazo[4,5-f][1,10]-phenanthroline)-bis(2,2'-bipyridine)-bis(hexafluorophosphate) 2. To a solution of *cis*-dichlorobis(2,2'-bipyridine)ruthenium(II) dihydrate

(0.1 g, 0.22 mmol) in ethanol (20 mL) was added **1** (89 mg, 0.22 mmol), and the reaction mixture was refluxed for 7 h. After cooling to room temperature, glacial acetic acid (three drops) and a solution of NH₄PF₆ (300 mg, 1.84 mmol) in water (10 mL) were added. The solution was boiled, partially concentrated, and cooled overnight in the fridge. The resulting precipitate was collected, washed with ether (10 mL), and dried under vacuum. The product obtained was dissolved in acetone (10 mL), and then hexane (10 mL) was added to induce the precipitation of the complex which was purified by crystallization from acetonitrile. Yield: 70%. Mp > 300 °C. ¹H NMR (400 MHz, acetone-*d*₆): δ 4.18 (s, 5H), 4.66 (st, 2H), 5.21 (st, 2H), 7.40 (t, 2H, *J* = 6.2 Hz), 7.63 (t, 2H, *J* = 6.2 Hz), 7.92 (m, 4H), 8.20 (m, 8H), 8.84 (t, 4H, *J* = 7.8 Hz), 9.07 (d, 2H, *J* = 7.8 Hz), 13.05 (s, 1H). ¹³C NMR (100 MHz, acetone-*d*₆): 68.5 (CH), 70.4 (CH), 71.1 (CH), 71.3 (q), 125.1 (q), 125.2 (CH), 126.8 (CH), 128.5 (q), 128.6 (CH), 131.4 (q), 131.6 (CH), 138.6 (CH), 138.8 (CH), 150.3 (CH), 150.7 (CH), 152.7 (CH), 158.0 (q), 158.2 (q). MS (FAB⁺): *m/z* (relative intensity): 1107 (100, M⁺+1). Anal. Calcd for C₄₃H₃₂F₁₂FeN₈P₂Ru: C, 46.63; H, 2.91; N, 10.12. Found: C, 46.41; H, 2.62; N, 10.34.

Acknowledgment. We gratefully acknowledge the financial support from MEC-Spain CTQ2004-02201 and Fundación Séneca (Agencia de Ciencia y Tecnología de la Región de Murcia) projects 02970/PI/05 and 04509/GERM/06 (Programa de Ayudas a Grupos de Excelencia de la Región de Murcia, Plan Regional de Ciencia y Tecnología 2007/2010). A.C. also thanks the Ministerio de Educación y Ciencia for a predoctoral grant.

Supporting Information Available: General comments. Computational details. NMR spectra. Electrochemical, UV–vis, fluorescence, ¹H- and ³¹P titration experiments. Electrospray mass spectra of complexed ligands. Reversibility experiments. Job's and detection limit plots. DFT calculated structures and NMR spectra. This material is available free of charge via the Internet at the <http://pubs.acs.org>.

JO800296C

(40) (a) Plitt, P.; Gross, D. E.; Lynch, V. M.; Sessler, J. L. *Chem.–Eur. J.* **2007**, *13*, 1374–1381. (b) Sessler, J. L.; Barkey, N. M.; Dan Pantos, G.; Lynch, V. M. *New J. Chem.* **2007**, *31*, 646–654.